

Supporting Information for:

Lanthanide Salen “Square Prism” and Wrapped Exo-lanthanide Salen “Double Decker”

Yu-Bo Shu and Wei-Sheng Liu*

Key Laboratory of Nonferrous Metals Chemistry and Resources Utilization of Gansu Province and State Key Laboratory of Applied Organic Chemistry, College of Chemistry and Chemical Engineering, Lanzhou University, Lanzhou, 730000, China. E-mail: liuws@lzu.edu.cn

Table of Contents

Experimental details

Figure S1 IR spectra

Figure S2 In-situ powder X-ray diffraction patterns of **1**

Figure S3 Powder X-ray diffraction patterns of **2**

Figure S4 Coordination geometries of Er(III) in **1** and **2**

Figure S5 Intermolecular π - π stacking (3.699 and 3.726 Å), van der Waals repulsion (3.528 Å), and van der Waals attraction (5.158 Å) in **1**

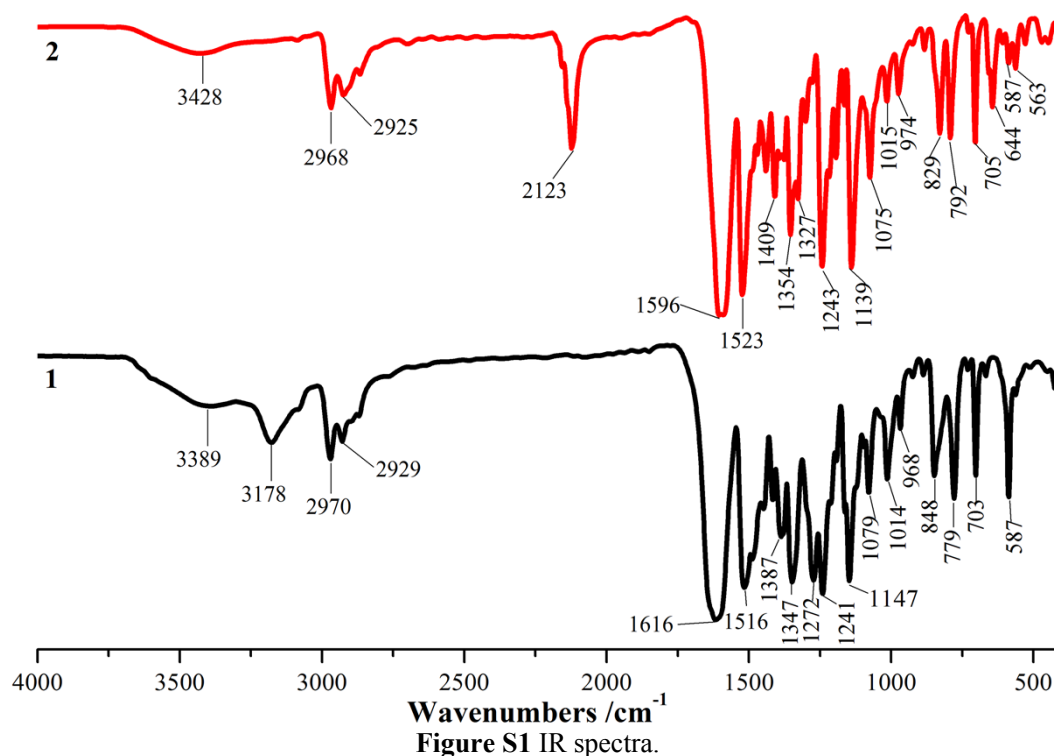
Figure S6 The 1-D array of “double decker” cations in **2**

Figure S7 TG curve of **1**

Figure S8 TG curve of **2**

Experimental details

All reagents were commercially available and were used without further purification. The H₂L ligand was synthesized by reaction of ethylenediamine (0.1202 g, 2 mmol) with 4-(diethylamino)salicylaldehyde (0.773 g, 4 mmol) in ethanol (30 mL) under reflux for 6 hours. Infrared spectra were recorded on a Nicolet FT-170SX instrument using KBr discs in the 400–4000 cm⁻¹ region. Powder X-Ray diffraction (PXRD) patterns were collected with a PANalytical X'Pert Pro Diffractometer operated at 40 kV and 40 mA with Cu *K*α radiation (step size: 0.0167113°, step time: 10.16 s). Elemental analyses were performed using an Elementar Analysensysteme GmbH varioEL cube instrument. Inductively coupled plasma-atomic emission spectroscopies (ICP-AES) analyses were carried out on an IRIS Advantage ER/S spectrophotometer. Thermal analyses were conducted using a PYRIS Diamond TG/DTA instrument. Reflectance spectra were recorded on a Shimadzu UV-2550 UV-Visible Spectrophotometer at room temperature. Steady-state excitation and emission spectra were recorded on FLS920 of Edinburgh Instrument at room temperature.



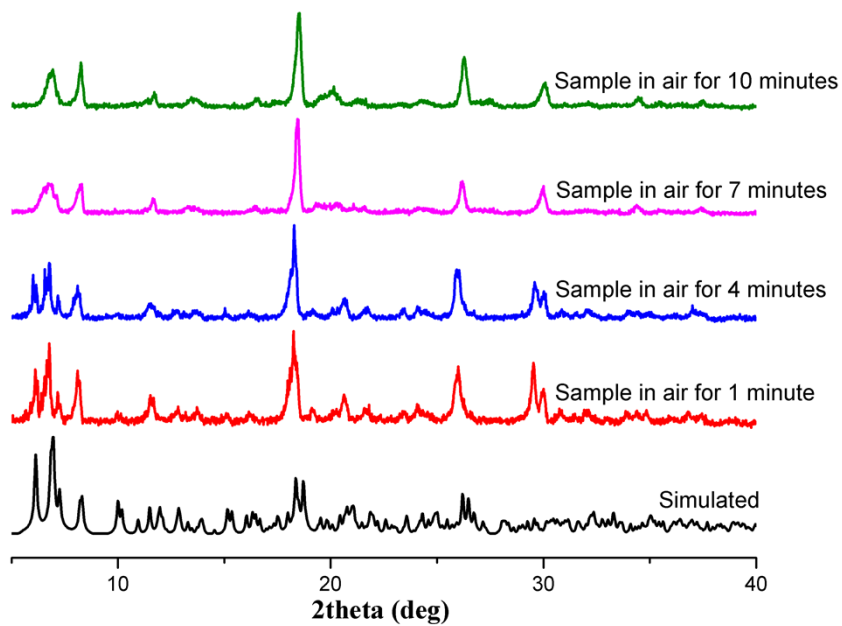


Figure S2 In-situ powder X-ray diffraction patterns of **1**.

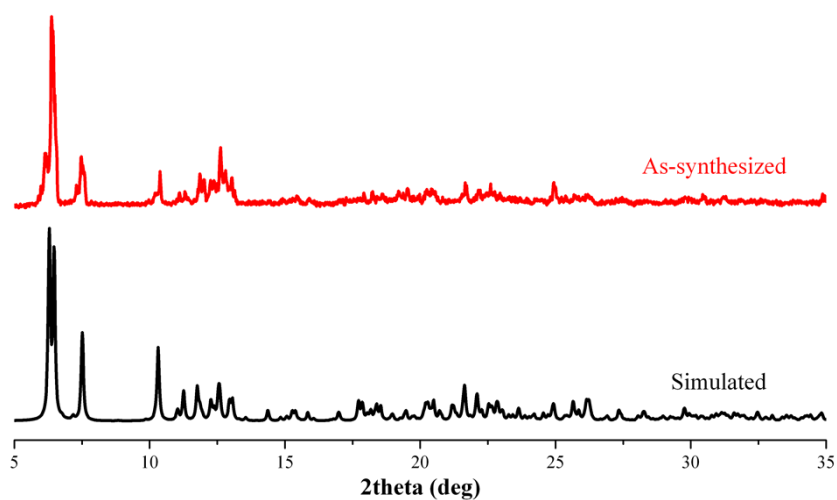


Figure S3 Powder X-ray diffraction patterns of **2**.

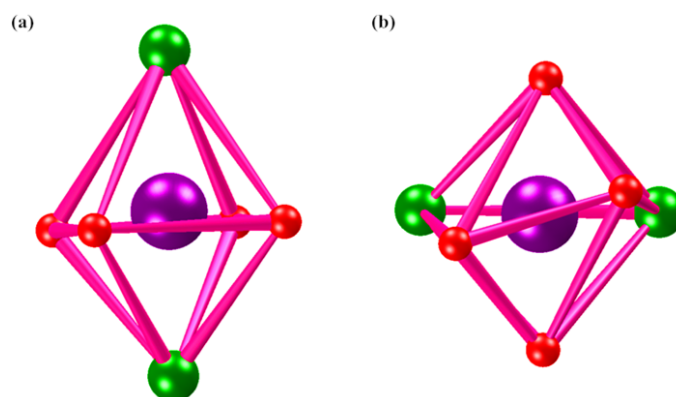


Figure S4 Coordination geometries of Er(III) in **1** (a) and **2** (b).

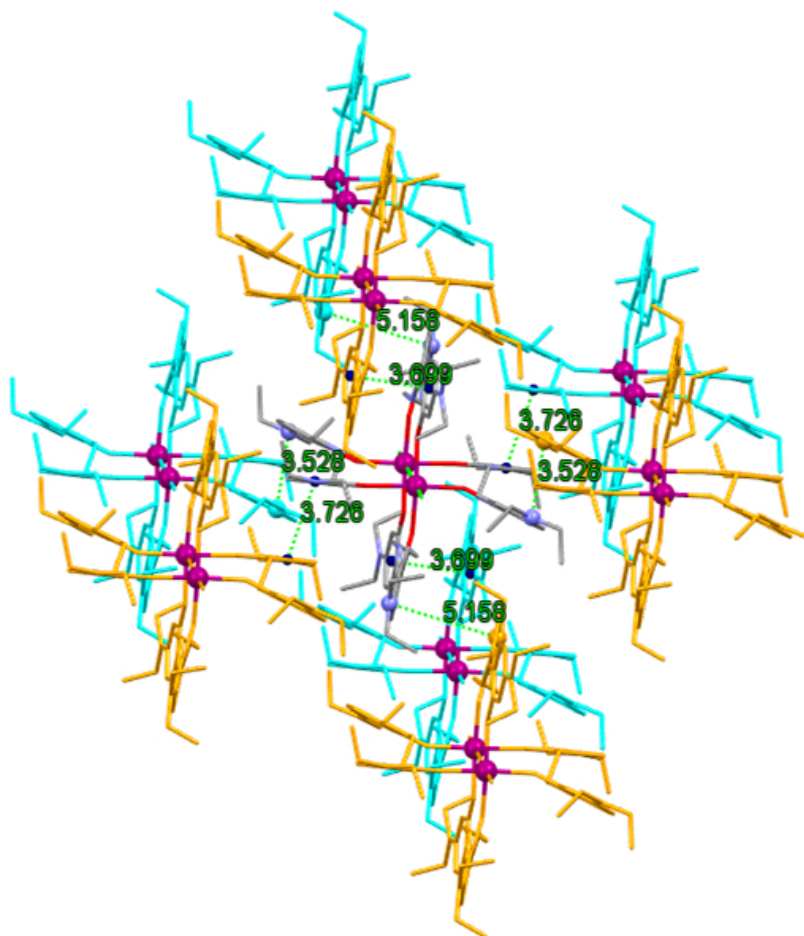


Figure S5 Intermolecular π - π stacking (3.699 and 3.726 Å), van der Waals repulsion (3.528 Å), and van der Waals attraction (5.158 Å) in **1**.

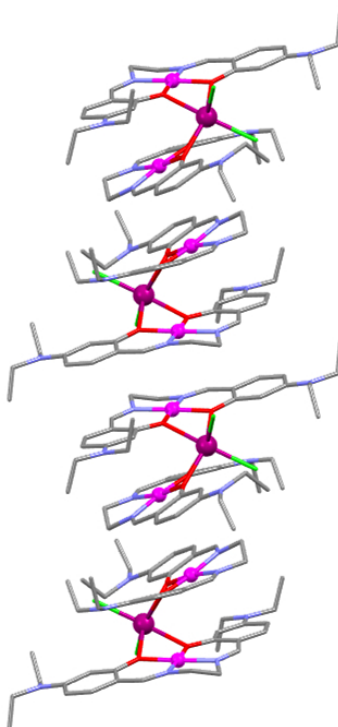


Figure S6 The 1-D array of "double-decker" cations in **2**.

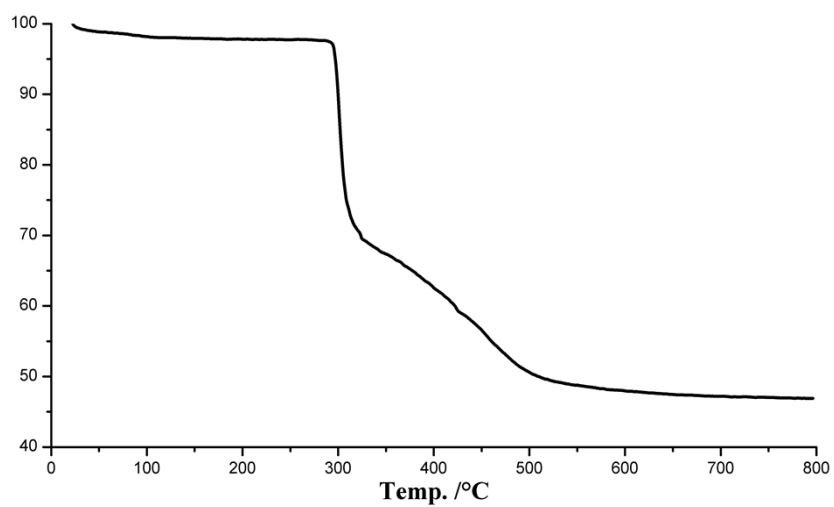


Figure S7 TG curve of 1.

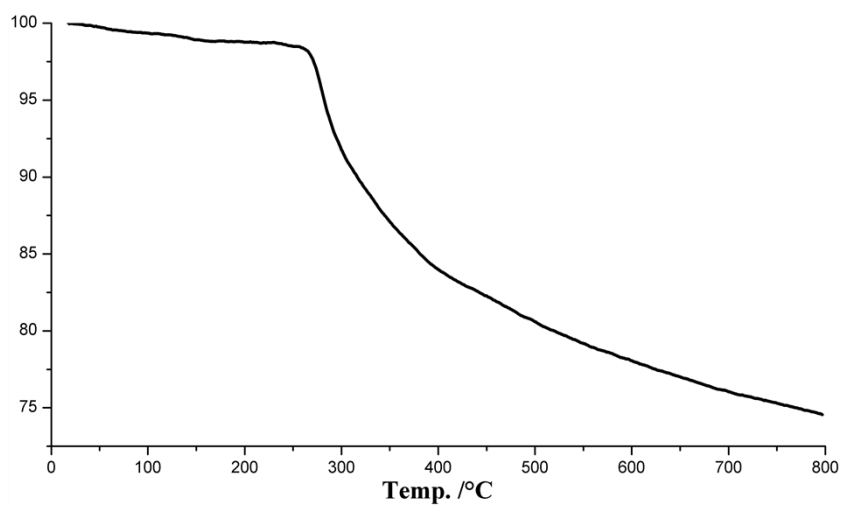


Figure S8 TG curve of 2.